



Resistance spot welding of dissimilar DP600 and DC54D steels

Xinjian Yuan ^{a,*}, Ci Li ^a, Jianbin Chen ^a, Xiuyang Li ^a, Xuebo Liang ^a, Xueyu Pan ^b

^a College of Materials Science and Engineering, Chongqing University, No. 174, Shazheng Street, Shapingba District, Chongqing 400044, PR China

^b Body Shop, Plant 2, Changan Ford Automobile Co., Ltd., No. 666, Jinshan Road, New Northern Zone, Chongqing 401122, PR China

ARTICLE INFO

Article history:

Received 3 February 2016

Received in revised form 10 August 2016

Accepted 10 August 2016

Available online 11 August 2016

Keywords:

Resistance spot welding

Advanced high strength steel

Transmission electron microscope

Electron back-scattered diffraction

Mechanical properties

Fracture mechanism

ABSTRACT

The microstructure in the fusion zone (FZ) was determined to be full lath martensite because of the high cooling rate. The heat-affected zone (HAZ) of DP600 was divided into coarse-grained, fine-grained, and inter-critical zones, and the volume fraction of martensite in HAZ was higher than that in the DP600 base metal (BM). The HAZ of DC54D was characterized by the presence of intensive ferrite. As the welding current, welding time, and electrode force increased, the tensile-shear strength of the welded spot experienced two stages of a notable increase and a subsequent decrease. The maximum value of 6.59 kN was obtained at a welding current of 9 kA, welding time of 14 cycles, and electrode force of 2.6 kN. Interfacial fracture occurred because of the small nugget diameter. Plug failure took place along the plastic deformed DC54D dominated by abnormally grown grains discovered from the interface of HAZ/BM through electron back-scattered diffraction.

© 2016 Elsevier B.V. All rights reserved.

1. Introduction

Advanced high-strength steels (AHSS) are increasingly applied in automotive industries for weight saving, safety consideration, and fuel efficiency. Wan et al. (2014) reported that AHSS possesses the potential to improve vehicle crash performance without increasing the weight because of the combination of excellent strength and formability. Zhang et al. (2009) indicated that the weight of an automobile can be reduced by 25% through the use of AHSS. Dual-phase (DP) steel, one of the most common AHSS, contains 5–20% hard martensite phase in a soft ferrite matrix and is mainly utilized as reinforcing parts in a white body (Ramazani et al., 2013). Ultra-low carbon extra-deep drawing steel DC54D is also widely used as auto body panels along with DP steels. The configurations of DC54D and DP steels are often involved in white body welding.

Resistance spot welding (RSW) is a well-known joining process for white body assembly; thousands of welded spots are required to complete the building of a white body. The performance of the structure thus depends not only on the mechanical properties of the sheets but also on the mechanical behaviors of the joints (Dancette et al., 2011). Pouranvari and Marashi (2010) investigated the mechanical performance of dual-phase DP600, DP780, and

DP980 grade steels and found that the softening of the heat-affected zone plays an important role in the mechanical properties of DP steels with a high volume fraction of martensite. Eshraghi et al. (2014) simulated the effect of parameters on the weld pool properties of DP600 through thermo-mechanical finite element analysis and indicated that current intensity is the key factor that affects the sizes of the molten and heat-affected zones. Zhang et al. (2014) investigated the RSW of a DP600/DP780 dissimilar couple and evaluated the macro-characteristics, microstructure, and mechanical properties of the welded joint and their relationship with welding parameters. Marashi et al. (2008) found that the welded spot in the pullout failure mode is controlled by the strength and size of the fusion zone (FZ) at the galvanized steel side; the hardness of FZ is governed by the dilution of the two base metals. Hayat (2011) analyzed the resistance spot weldability of 180-grade bake hardening steel and 7123-grade interstitial free steel and found that failure occurs at the 7123-grade interstitial free steel side. The weldability of high-strength steel is one of the key factors governing its application in RSW, as demonstrated by Hwang et al. (2011). Welding with unequal thickness and dissimilar metals is significantly different from welding with equal thickness and similar metals. Thus, large gaps in physical, chemical, mechanical properties, and microstructure exist. The studies cited above indicate that although numerous investigations have been conducted on the welding of automobile steels, most of these investigations focused on the welding of steels with equal thickness and similar microstructural characteristics. The welding of dissimilar sheets with different thickness values

* Corresponding author.

E-mail addresses: xinjianyuan@yahoo.com, xinjianyuan@cqu.edu.cn, cqu.y@sina.com.cn (X. Yuan).



Table 1

Chemical composition and mechanical properties of DP600 and DC54D.

Chemical composition (wt.%)							Ultimate tensile strength (MP)	Elongation (%)
Steel	C	Mn	Si	Cr	Nb	Mo		
DP600.	0.10	0.4	0.14	0.16	–	0.18	600	23
DC54D	0.002	0.16	–	0.01	0.02	–	160	44.6

has been rarely reported despite the high practical significance of these steels.

To address this issue, DP steel DP600 and ultra-low carbon steel DC54D were joined as a dissimilar couple through RSW in the current study. Two significant aspects were highlighted. First, in-depth characterization of the joint microstructure was conducted through optical microscopy (OM), scanning electron microscopy (SEM), electron back-scattered diffraction (EBSD), and transmission electron microscopy (TEM). Second, the relations between microstructure and mechanical properties as well as the fracture mechanisms were discussed comprehensively.

2. Experimental procedure

Ultra-low carbon steel DC54D containing a ferritic phase with a thickness of 1.0 mm and galvanized DP600 exhibiting a ferrite–martensite DP with a thickness of 1.6 mm were used as the base metals (BMs). The chemical composition and mechanical properties of DP600 and DC54D are shown in Table 1.

RSW was implemented using an OBARA SIV21 spot welding machine with a Cu–Cr–Zr alloyed electrode with 6 mm diameter. One sample for metallographic analysis and three samples for tensile-shear testing were welded per welding parameter. The weld was at the center of two identical single-lapped 30 mm × 30 mm DP600 and DC54D steel sheets. Fig. 1 shows the schematic of RSW and tensile-shear testing. The tensile direction is in accordance with the rolling direction.

Macro photographs were captured with a digital camera. The welded spots were sectioned across the center line by wire-electrode cutting. The samples were ground with silicon carbide paper and etched via corrosion with 2% Natal for about 15 s at room temperature. The nugget diameters and depth of indentation were obtained from the resultant metallograph.

The microstructures of the welded joints were analyzed through OM and SEM (TESCAN VEGA 3 LMH, Czech) at a voltage of 20 kV. Furthermore, the phase and grain size of FZ and the heat-affected zone (HAZ) were investigated through EBSD and TEM (FEI TECNAI F20, America) at a voltage of 200 kV. Thin foils of jet-polished samples were produced for TEM. The hardness profiles in transverse and vertical directions were measured with a Vickers hardness tester (MH3N) with a load of 300 g and a dwelling time of 10 s. The indentations were spaced 0.2 mm apart. The tensile-shear properties of the welded joints were determined with a SANS microprocessor-controlled servo hydraulic universal testing machine with a travel speed of 2 mm min⁻¹.

3. Results and discussion

3.1. Macro characteristics of welded joints

Fig. 2 shows macro photographs of resistance-spot-welded joints at different welding currents, welding times, and electrode force. Significant differences were observed under various welding parameters. The welding surfaces for the different welding parameters are shown in different colors. When the welding current exceeded 9 kA or the welding time was more than 11 cycles, the welding surfaces exhibited the color of canary yellow because of the reaction between the zinc coating and copper electrode according to Hayat (2011). Small burrs originating from expulsion were found in several welded spots. In contrast with DC54D, expulsion emerged easier in DP600.

Fig. 3 shows the relationship between the macro characteristics of DP600/DC54D welded spots and the key welding parameters. Figs. 2a and 3a show that the nugget diameter increased from 5.58 mm to 7.80 mm as the welding current increased from 6 kA to 11 kA. Figs. 2b and 3b show that the influence of welding time (5–20 cycles) on nugget diameter was similar to that on welding current.

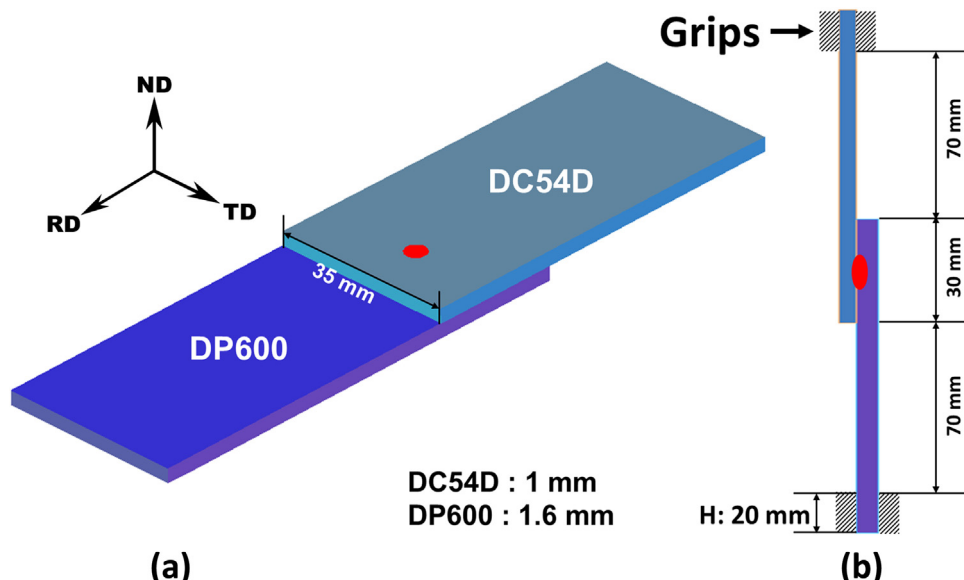


Fig. 1. Configurations of steel sheets: (a) during RSW and (b) during tensile-shear testing.

Download English Version:

<https://daneshyari.com/en/article/792811>

Download Persian Version:

<https://daneshyari.com/article/792811>

[Daneshyari.com](https://daneshyari.com)